Arch Environ Contam Toxicol (2008) 55:372–385
DOI 10.1007/s00244-008-9135-4

Effects of Deposition of Heavy-Metal-Polluted Harbor Mud on Microbial Diversity and Metal Resistance in Sandy Marine Sediments

Ann-Charlotte M. Toes · Niko Finke · J. Gijs Kuenen · Gerard Muyzer

Received: 6 August 2007 / Accepted: 21 January 2008 / Published online: 14 February 2008

Abstract Deposition of dredged harbor sediments in relatively undisturbed ecosystems is often considered a viable option for confinement of pollutants and possible natural attenuation. This study investigated the effects of deposition of heavy-metal-polluted sludge on the microbial diversity of sandy sediments during 12 months of mesocosm incubation. Geochemical analyses showed an initial increase in pore-water metal concentrations, which subsided after 3 months of incubation. No influence of the deposited sediment was observed in denaturing gradient gel electrophoresis (DGGE) profiles of bacterial 16S rRNA genes, whereas a minor, transient impact on the archaeal community was revealed. Phylogenetic analyses of bacterial 16S rRNA clone libraries showed an abundance of members of the *Flavobacteriaceae*, the α- and γ-*Proteobacteria*, in both the muddy and the sandy sediments. Despite the finding that some groups of clones were shared between the metal-impacted sandy sediment and the harbor control, comparative analyses showed that the two sediments were significantly different in community composition. Consequences of redeposition of metal-polluted sediment were primarily underlined with cultivation-dependent techniques. Toxicity tests showed that the percentage of Cd- and Cu-tolerant aerobic heterotrophs was highest among isolates from the sandy sediment with metal-polluted mud on top.

A.-C. M. Toes · J. G. Kuenen · G. Muyzer (✉)
Department of Biotechnology, Delft University of Technology, Julianalaan 67, NL-2628, BC, Delft, The Netherlands
e-mail: g.muyzer@tudelft.nl

N. Finke
Max Planck Institute for Marine Microbiology, Celsiusstrasse 1, 28359 Bremen, Germany

Introduction

Different degrees of heavy metal pollution have been observed in coastal areas of northwestern Europe, mostly attributed to industrial discharges, waste-disposal streams, and atmospheric deposition of exhaust gasses. Stringent environmental legislation has led to a reduction of these metal discharges in the last 15 years (EEA 2003). However, considerable heavy metal pollution of sediments from harbors and marinas have been attributed to the application of antifouling paints on ship hulls (Schiff et al. 2004; Warnken et al. 2004). Some of these harbors have to be dredged frequently for navigational purposes, as is the case for harbors in northwestern Europe, from which more than 200 million cubic meters of contaminated sludge is dredged on an annual basis (Bortone et al. 2004). Dredging operations can increase metal mobilization by whirling up fine-sediment particles and allowing oxygen to come in contact with previously buried and reduced sediments. The extent of metal release depends on local parameters such as sediment geochemistry, currents, grain size, pH, and salinity (Van den Berg et al. 2001). Unquestionably, a variety of biological parameters also play a role in metal mobilization.

When sediment contamination is low, several methods are available to avoid (potential) dispersion or release of toxic metals. Risk assessment studies show that *in situ* capping (confinement by an inert barrier) or passive natural attenuation offer viable alternatives to removal of sediments by dredging (Wang et al. 2004). However, when metal-contaminated sediments need to be removed for navigational purposes, the most common practice is to simply relocate the dredged material in the same system, with the assumption that this procedure has minimal effect on biotic and abiotic parameters (Bortone et al. 2004) and, hence, will not lead to the release of toxic metals. This study therefore investigated

the effect of the deposition of dredged metal-contaminated sediment on microbial diversity and metal resistance of microbes in uncontaminated sandy sediment.

Bacterial heavy-metal-resistances studies have been carried out mostly on pure cultures (Miao et al. 2005; Nies 1999; Silver 1996; Surosz and Palinska 2004). Recently, some insight has also been gained into the genetic flexibility of mixed microbial populations with respect to metal contamination and widespread occurrence of lateral gene transfer in response to metal toxicity (Cook et al. 2001; Sobecky et al. 1998). Whereas effects on phytoplankton and archaeal communities are described, most studies have focused on bacterial diversity in marine sediments with long-term impact by heavy metals (Gillan et al. 2005; Powell et al. 2003; Sorci et al. 1999). An investigation of biodiversity in several polluted and pristine Antarctic sediments showed substantial statistical variation between and within control groups (Powell et al. 2003). Furthermore, although Sorci and co-authors (1999) observed an increase in biodiversity along with heavy metal contamination, other investigators measured no change (Gillan et al. 2005) or the exact opposite response (Sandaa et al. 1999a). These differences might be explained by adaptation time and/or cocontamination with organic material, but these assumptions remain speculative. Therefore, this study was limited to better controlled conditions. We used (relatively) short-term exposure to metals and employed mesocosms in order to minimize abiotic variances and to enable frequent sampling.

We describe the effects of controlled disturbance ("dredging") and redeposition of metal-polluted silty sediment on a sandy sediment, by combining diversity assessments of Bacteria, Archaea, and Cyanobacteria with temporal and spatial profiles of metals. Four mesocosms were subjected to selected treatments mimicking the deposition of metal-polluted sediment, microscale disturbances (i.e., bioturbation by *Nereis diversicolor*), and seasonal variation (i.e., algal bloom by the addition of *Spirulina* sp.). Geochemical analyses of the sediments comprised measurements of nutrients, oxygen, and heavy metals throughout the duration of the project (16 months). Microbial diversity studies focused on the first 2 cm of surface sediments and included 16S rDNA DGGE (denaturing gradient gel electrophoresis) analysis for the domains Bacteria and Archaea, as well as for the phylum Cyanobacteria. Bacterial diversity was further explored by the construction of 16S rDNA gene clone libraries and metal-toxicity tests on aerobic heterotrophic isolates.

Materials and Methods

Description of Field Sites

In June 2003, intact blocks of sediment were collected from a metal-contaminated harbor basin (HB) and a geographically related intertidal flat (IF) on the North Sea coast of Germany. The HB sediment was sampled at a 11-m depth with a box-corer and was composed primarily of fine-grained material (78.6% of the grains were smaller than 20 μm). Hydrocarbon contamination was detected in the harbor sediment (polychlorinated biphenyl: 41–175 μg/kg dry weight; and polyaromatic hydrocarbon: 14–18mg/kg dry weight).

The sediment from the IF was composed mainly of coarser grains (99.5% of the grains ranging from 200 to 600 μm; M. Huettel, personal communication). Salinities in the HB and the IF were low (28‰ and 29–30‰, respectively), reflecting the input of freshwater from a river situated 3 km west of the harbor region. The IF sampling site has been described elsewhere (de Beer et al. 2005; Musat et al. 2006).

Mesocosm Design, Treatments, and Sampling

For controlled and time dependent measurements, mesocosms were set up and run during the duration of the project (16 months, June 2003–October 2004). Four glass aquaria, each 120 × 30 × 20 cm, were filled with sediments (36 L, or ~38.5 kg dry weight of IF sediment and 21.9 kg dry weight of HB sediment) to a height of 10 cm. The mesocosms were filled with North Sea water, resulting in a water column of 10 cm on top of the sediment (36 L). Four mesocosms were established with (1) polluted sediment (HBC), (2) homogenized polluted sediment (HBH), (3) sandy sediment (IFC), and (4) sandy sediment with a 3-mm layer of polluted sediment deposited on top (IFD).

Water (salinity 27–30‰) was permanently circulated with a metal-free pump at flow rates ranging from 9 to 10.5 cm/s. In order to compensate for evaporation, deionized water was added when necessary. The mesocosms were kept at constant temperature (19°C) and illuminated 12 h per day with fluorescent tubes (T5/Biolight, daylight 80W), at a total irradiance of 40–50 μmol photons/m/s at the sediment surface. Measurements of pH in the water column of the mesocosms showed little variation over time [i.e., 8.0 ± 0.1 (HBC and HBH) and 7.8 ± 0.1 (IFC and IFD)].

Mesocosm HBC contained undisturbed sediment from an industrial HB. Sediment from the same location was homogenized in a cement mixer for 20 min under aerobic conditions before being placed in mesocosm HBH, mimicking mixing processes that might occur during dredging. Mesocosms IFC and IFD contained sediments from an IF of the German Wadden island Sylt. After an initial stabilization period of 3 months (June 2003–October 2003), 1 L of metal-contaminated sediment was added to mesocosm IFD in October 2003, forming a layer of about 3 mm

thickness on the sediment surface. In November 2003, bioturbation was introduced in all sediments by the addition of 100 individuals of the polychaete *N. diversicolor*. In February 2004, a spring algal bloom was mimicked by the addition of organic matter (30 g C/m^2) in the form of algae [80% dried *Spirulina* sp. (Aldrich) and 20% macroalgae collected from a beach]. In September 2004, an additional 50–80 individuals of *N. diversicolor* and *Arenicola marina* were added to each mesocosm. Survival time of the polychaete worms in mesocosms HBC and HBH varied from 2 to 5 months, whereas in mesocosms IFC and IFD, they lasted throughout the project.

Samples for DNA extraction as well as samples for the culture-dependent experiments were taken from the top 2 cm of surface sediment with sterile, cutoff syringes (2.5 mL). In all cases, samples from three different points in the mesocosms were taken and pooled together, in order to minimize variation due to heterogeneity.

Pore-Water Carbon, Nutrients, Oxygen, and Metal Analysis

Pore water was extracted by centrifugation of the sediment (sampled with a small corer, 2.6 cm in diameter, and 1-cm-thick slices resulting in 5.3 mL of sediment) in acid-washed Spinex™ (Phenomenex) filter units at 2500*g* for 10 min. Samples for nitrate, ammonia, phosphate, and silicate were measured as described previously (Hansen and Koroleff 1999). Sulfate concentrations were measured with an ion chromatograph (Ferdelmann et al. 1997). Total carbon (TC) and total organic carbon (TOC) were measured in freeze-dried sediment samples with the CNS Analyzer (Fisons Eager 200). For the TOC measurements, the samples were acidified with 6 N HCl prior to analysis to release inorganic carbon. Oxygen consumption and production rates were determined from the change of the oxygen concentration in the water column. The mesocosms were closed without gas phase and the water column oxygen concentration during light and dark incubation was monitored with oxygen microoptodes (Microx TX3; Presense). For determination of pore-water metal concentrations, samples were amended with 100 μL of 12 N HCl to prevent oxidation of the metal. The samples were centrifuged and the supernatant was stored at 4°C until analysis on the inductively coupled plasma–mass spectrometer (ICP-MS; Zhang and Davison 1999). A certified reference material (SLRS-4 from the National Research Council of Canada) was measured routinely. The values obtained were within the standard deviation of the certified values. The diffusive flux of dissolved constituents across the sediment–water interface can be calculated according to Fick's first law of diffusion with a modification appropriate for sediments. In this work, metal fluxes were calculated for each mesocosm using the concentration gradient of DET (diffusive equilibrium thin gel technique; Zhang and Davison 1999) metal measurements over a 4-mm distance immediately below the sediment surface. Diffusive gels were prepared using acrylamide solution and an agarose derivative crosslinker (DGT Research Ltd), as described by Zhang and co-authors (1995). DET probes were deployed for 56 h in the sediment. Nonlinearity in some concentration gradients could introduce errors in some calculations.

Cultivation of Heterotrophic Bacteria and Metal Toxicity Assay

Filter-sterilized mesocosm water (5 mL) was added to pooled sediment samples (~6 g wet sediment) and shaken rigorously for 10 min. Of this solution, 10, 25, and 50 μL were used to inoculate agar plates containing a mineral medium (1 L contained the following: 1 g NH_4Cl, 0.2 g $MgSO_4 \cdot H_2O$, 0.1 g $CaCl_2 \cdot 2H_2O$, 0.05 g $K_2HPO_4 \cdot 3 H_2O$, 27.5 g NaCl, 10 mmol HEPES, 5 mmol acetate, 10 mg yeast extract, 1 mL of standard trace element solution, and 15 g agarose, pH 7.5; Widdel and Pfennig, 1984). After 24 h of incubation at 25°C, individual colonies were picked with sterile toothpicks and used as inoculum for new plates, until 30 monoclonal ("pure") cultures per mesocosm were obtained (excluding mesocosm HBH because initial experiments did not indicate any differences with HBC). Due to the presence of isolates with agarolytic traits in collections from IFC and IFD, fewer isolates could be tested on agar diffusion assays (i.e., 21 and 23, respectively).

Isolates were subjected to zone of inhibition assays with filter disks impregnated with either 500 nmol of $CuSO_4$ or 150 nmol of $CdCl_2$ in duplicate. Previous tests with variable amounts of Cu and Cd on impregnated disks showed that the applied concentrations resulted in an adequate separation of tolerant and sensitive bacterial species. Plates were incubated at 25°C for 72 h prior to measuring the zone of growth inhibition with a ruler. Bacteria were identified as metal tolerant when growth occurred within a 5-mm zone of the center of the Petri dish and as metal sensitive when zone of growth inhibition was larger than 12 mm.

DNA Extraction and 16S rRNA Gene Amplification

Extraction of genomic DNA was performed on sediment samples (0.25–0.5 g of wet sediment) with the Ultra Clean Soil DNA Isolation Kit (MoBIO Laboratories, USA) according to the manufacturer's manual. Genomic DNA was used for amplification of DGGE fragments and the nearly complete bacterial 16S rRNA gene. All polymerase chain reaction (PCR) reactions were conducted in 50-μL

reactions with ~50 ng target DNA using the *Taq* PCR Master Mix kit (QIAGEN, Germany) in a Thermocycler (BioMetra, Germany). PCR products were analyzed by gel electrophoresis (1% agarose gel, 30 min, 100 V), stained with ethidium bromide (0.6 μg/mL) and visualized with the Bio-Rad Gel Doc 1000 under ultraviolet (UV) illumination.

Bacterial DGGE fragments were amplified as described previously with primers 341F-GC and 907R (Schäfer and Muyzer 2001). DGGE fragments from Cyanobacteria and chloroplasts were amplified with primer 359F-GC and an equimolar mixture of the reverse primers 781R(a) and 781R(b) and PCR conditions as described by Nübel et al. (1997). DGGE fragments of Archaea were amplified with primers Parch519F and ARC915R-GC and PCR conditions as described previously (Coolen et al. 2004).

The nearly complete bacterial 16S rRNA genes were amplified with forward primer 63f-mod and reverse primer 1387r-mod (Marchesi and Weightman 2000). The PCR reactions were conducted according to the following program: 94°C for 5 min (1 cycle), 94°C for 1 min, 65°C for 1 min, 72°C for 3 min (30 cycles), and final extension at 72°C for 10 min (3 cycles).

DGGE and MDS Analyses

Denaturing gradient gel electrophoresis was performed as described previously (Schäfer and Muyzer 2001). Approximately 400 ng of PCR product was loaded per lane. For the analysis of Bacteria and Cyanobacteria, gels with denaturant gradients of 20–80% were run for 16 h at 100 V. The archaeal community was analyzed by running gels with a 20–60% denaturing gradient for 5 h at 200 V. Gels were incubated for 30 min in an ethidium bromide solution (0.5 μg/mL) and photographed using the GelDoc UV Transilluminator. In order to assess changes in the microbial communities over time, the DGGE patterns were analyzed with multidimensional scaling (MDS) as described previously (Schauer et al. 2000). Digital DGGE images were analyzed with an ImageJ 1.36b (Wayne Rasband, National Institutes of Health, USA; http://www.rsb.info.nih.gov/ij). This program creates a density profile through each lane, detecting bands and their intensity. For each DGGE gel, these values were used to create a species-abundance matrix, which was imported into the statistical program Primer-E (version 6, UK Department for Environment, Food and Rural Affairs). Data were standardized by applying a square root transformation, after which a resemblance matrix was created using Bray-Curtis similarity. MDS configuration plots were generated and these graphs received an overlay of cluster analysis of the same samples (based on similarity, chosen percentages of 50%, 60%, and 75%).

Clone Libraries and Screening

Three clone libraries were prepared with near-complete 16S rRNA genes amplified from mesocosm HBC (May 2004 and October 2004, HBC_2 and HBC_3, respectively) and from mesocosm IFD (October 2004, IFD_3). Initially, the PCR product was purified by gel electrophoresis [2% (w/v) agarose gel], excised and processed with the QIAquick Gel Extraction Kit (QIAGEN, Germany). The PCR product was ligated in the PCR 2.1-TOPO® vector and used to transform TOP10 chemically competent *Escherichia coli* cells, according to the manufacturer's manual (Invitrogen Life Technologies, The Netherlands). Of the positive clones 38, 101 and 103, clones from HBC_2, HBC_3, and IFD_3, respectively, were subjected to colony PCR of the insert using primers 63f-ext and 1387r-ext (Marchesi and Weightman 2000). ARDRA screening (amplified ribosomal DNA restriction analysis) with restriction enzyme *Rsa*I was done at 37°C for 2 h. Restriction products were separated by gel electrophoresis [2% (w/v) agarose gel, 180 min, 80 V], stained and visualized as described earlier. The restriction patterns were clustered manually. Of each cluster, two to four representative clones (except for groups with only one representative) were selected for complete sequencing of the insert. Plasmids of selected clones were purified with the QIAprep Spin Miniprep Kit (QIAGEN, Germany).

Sequencing, Phylogenetic Analysis, and Accession Numbers

Insert-containing plasmids were sequenced with universal primers M13 forward (-20) (5′-GTA AAA CGA CGG CCA G-3′), M13 reverse (5′-CAG GAA ACA GCT ATG AC-3′), and internal primer 907R. Excised, reamplified, and purified DGGE bands were sequenced with the appropriate forward primer, lacking the GC-clamp. All DNA sequencing reactions were carried out on an ABI 3730 sequencer (Applied Biosystems, USA). Partial clonal sequences were combined in the Web-based program CAP sequence assembly machine to form a contig (http://www.bio.ifom-firc.it/ASSEMBLY), of which the remaining primer sites were removed. Modified sequences were compared to sequences stored in GenBank using the BLAST algorithm (Altschul et al. 1990; http://www.ncbi.nlm.nih.gov/BLAST) and subsequently imported into the ARB software program (Ludwig et al. 2004; http://www.arb-home.de). Alignments were corrected manually when necessary. A phylogenetic tree was created with the neighbor-joining algorithm. Shorter sequences, such as the DGGE bands, were inserted into this tree one at a time while applying a filter focusing only on the positions of the shorter fragment. Clonal 16S rRNA sequences were

deposited at GenBank under accession numbers DQ334608 to DQ334670 and EF137898 to EF137903. Excised, reamplified, and identified DGGE bands were deposited under accession numbers EF137873 to EF137897.

WebLIBSHUFF Analysis and Calculation of Diversity Indexes

A similarity matrix, calculated with Jukes–Cantor correction, was exported from ARB software and used to estimate coverage curves and comparisons between clone libraries with the Web-based program webLIBSHUFF (J. R. Henriksen, 2004; http://www.libshuff.mib.uga.edu/) From this similarity index, a species-abundance file was created by grouping similarity coefficients higher than 95% (chosen OTU definition). Multiplication with the corresponding frequency of the ARDRA cluster gave rise to species-abundance data. This file was used as input for EstimateS, a Web-based program that allows for the determination of several nonparametric biodiversity estimators (Version 7.5, R. K. Colwell, http://www.purl.oclc.org/estimates). Diversity settings included the use of the classical formula for the Chao2 estimator, setting the sample randomization to 1 and putting the upper abundance limit for rare species to 3. Coverage was calculated using the method of Good (Good 1953) with the equation $C = (1 - (n_1/N)) \times 100$, where n_1 is the number of unique clones within a library and N is the total number of clones examined. Coverage of clone libraries is a parameter that gives information about how well the retrieved data resemble the original sample, by using statistical information on the frequencies of rare clones. Richness estimators are used to compare biodiversity between different samples and take into account both the number of species and their relative abundance.

Results

Sediment Characterization and Mesocosm Incubation

Two marine sediments were used in this study (i.e., metal-polluted, fine-grained sediment from a HB and sandy sediment from a relatively undisturbed IF) (Table 1). Four mesocosms were established with (1) polluted sediment (HBC), (2) homogenized polluted sediment (HBH), (3) sandy sediment (IFC), and (4) sandy sediment with a 3-mm layer of polluted sediment deposited on top (IFD). A description of the four mesocosms, incubation conditions, and specific treatments is presented in the Materials and Methods section. Pore-water concentrations of ammonia, phosphate, sulfate, and carbon content were measured during mesocosm incubation in order to investigate the impact of experimental disturbances on abiotic parameters. Oxygen fluxes were measured at the sediment–surface interface as an indirect indicator of (photosynthetic) microbial activity. Table 1 summarizes geochemical characteristics of the sediments in the mesocosms at different time points: after 3 months in the mesoscosms, directly following the deposition of metal-polluted silt on the sandy sediment in mesocosm IFD (October 2003), again 3 months later, well after the introduction of bioturbation (January 2004), and after 1 year of mesocosm incubation (October 2004). TC remained more or less stable during incubation in the mesocosms. Homogenization and redeposition of polluted muddy sediment (mesocosms HBH and IFD) had minor effects on organic carbon when compared to the control mesocosms (HBC and IFC, respectively). Ammonia concentrations were elevated in the homogenized polluted sediment (HBH) and remained high after 1 year.

Illumination during daytime resulted in the development of a dense cover of phototrophic biomass in mesocosm IFC and to a lesser extent in IFD. The oxygen penetration depth generally varied between 2 and 8 mm in all sediments. Oxygen fluxes were measured regularly at the sediment–

Table 1 Carbon and nutrients in surface sediments (top 2 cm)

Nutrient	Time	Mesocosm			
		HBC	HBH	IFC	IFD
TC (in mmol C/g dry weight)	Oct. 2003	3.5	3.4	0.11	0.11
	Jan. 2004	3.4	3.4	0.12	0.13
	Oct. 2004	3.3	3.1	0.27	0.12
TOC (in mmol C/g dry weight)	Oct. 2003	1.10	0.74	0.03	0.08
	Jan. 2004	89	0.94	0.04	0.10
	Oct. 2004	0.86	0.76	0.03	0.05
C/N (total C/total N)	Oct. 2003	11.3	11.5	6.1	7.4
	Jan. 2004	10.7	10.6	6.6	7.0
	Oct. 2004	10.5	10.9	7.2	5.8
NH_4^+ (in μM)	Oct. 2003	51	110	ND[a]	ND
	Jan. 2004	55	88	58	31
	Oct. 2004	43	79	15	19
PO_4^{3-} (in μM)	Oct. 2003	30	8.3	ND	ND
	Jan. 2004	15	12	11	9.4
	Oct. 2004	15	11	13	26
SO_4^{2-} (in mM)	Oct. 2003	25	23	29	27
	Jan. 2004	23	20	26	25
	Oct. 2004	24	28	22	24

Note: HBC: undisturbed harbor sediment; HBH: homogenized harbor sediment; IFC: undisturbed intertidal sediment; IFD: intertidal sediment with a 3-mm layer of HBH deposited on top. Oct. 2003: samples taken directly after sediment deposition in IFD; Jan. 2004: samples taken after bioturbation was introduced; Oct. 2004: samples taken after introduction of organic matter and renewed bioturbation

[a] ND: not determined

water interface in the mesocosms. Oxygen fluxes in the control sandy mesocosm (IFC) remained quite stable for the first 3 months, at around 10 mmol O_2/m^2/day (a positive number indicating transport from sediment to water column), and then steadily increased to 72 mmol O_2/m^2/day in October 2004. In contrast, oxygen production declined rapidly in mesocosm IFD after deposition of silt on the sandy sediment: 22 mmol O_2/m^2/daylight in September 2003, to 4 mmol O_2/m^2/daylight in November 2003, and dropping to zero in January 2004. In mesocosms HBC and HBH, oxygen production was stable in time, but data indicated lower oxygen production rates (i.e., 7 mmol and 5 mmol O_2/m^2/daylight, respectively).

Metal Analysis

Spatial and temporal concentration profiles of Fe, Cu, and Cd in the mesocosm sediments were measured in order to estimate the extent of metal release or metal immobilization during controlled disturbances. In Figure 1 pore-water concentrations of Fe (Figs. 1A and 1B), Cu (Figs. 1C and 1D), and Cd (Figs. 1E and 1F) in the sediments directly after deposition of metal-polluted sediment in IFD (October 2003) and after 6 months of mesocosm incubation with bioturbation (January 2004) are summarized. Please note that the units of the *x*-axis in the right-hand panels are a factor 3–10 lower than the left-hand panels. From the first pore-water profiles (Figs. 1A and 1B), it can be seen that Fe dominated metal geochemistry in HB sediments and was detected at all depths of the sediment column. The sandy IF sediments had Fe concentrations approximately threefold to fivefold lower, with the exception of the October 2003 IFD sample, taken directly after metal-polluted mud deposition, showing considerable Fe concentrations below a 3-cm depth. Regarding Cu and Cd, pore-water concentrations were elevated in sediment IFD in October 2003 (Figs. 1C and 1E, respectively), whereas after 3 months, levels were back to the control values (Figs. 1D and 1F, respectively). Both Cu and Cd profiles show maximal concentrations at, or just below, the sediment surface.

Microscale pore-water metal analysis at the sediment–water interface measured with DET permitted the estimation of metal fluxes as presented in Table 2. Initially, substantial metal fluxes could be measured (i.e., from sediment into water column) in mesocosms HBC and IFD. After 3 months of bioturbation, most metal fluxes had subsided, except for Cu, which was relatively high at the end of the project. The homogenized sediment in mesocosm HBH initially exhibited little or no metal fluxes, but metal transport developed after 3 months and then declined.

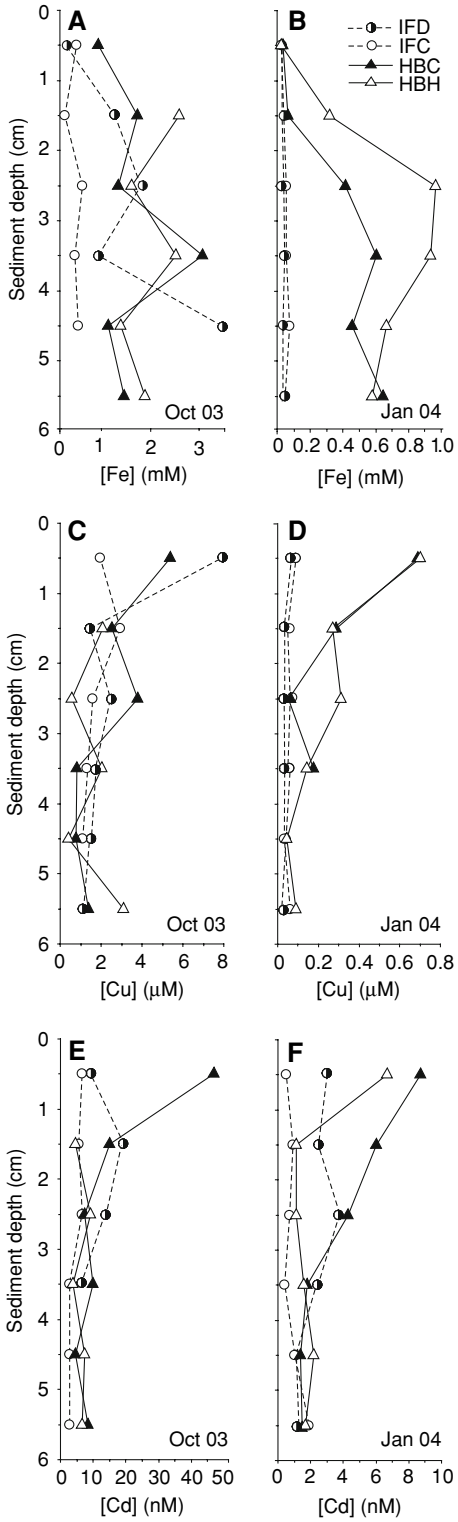

Fig. 1 Pore-water Fe **(A, B),** Cu **(C, D)**, and Cd **(E, F)** concentrations in mesocosm sediment during incubation (two replicates). Symbols shown in part B are valid for all graphs. Note that the scales of the *x*-axes of all right-hand panels are a factor 3–10 lower. Timing as described in legend of Table 1. Error bars were smaller than symbols

Table 2 Estimated metal fluxes across the sediment–water interface for Fe, Cu, and Cd during mesocosm incubation

Metal flux[a]	Time	Mesocosm			
		HBC	HBH	IFC	IFD
Fe flux (μmol/m^2/day)	Oct. 2003	980	20	ND[b]	2300
	Jan. 2004	90	1600	−4	−20
	Oct. 2004	−28	90	−21	44
Cd flux (nmol/m^2/day)	Oct. 2003	0	−5	ND	160
	Jan. 2004	0	−4	13	−3
	Oct. 2004	−4	3	0	0
Cu flux (nmol/m^2/day)	Oct. 2003	ND	ND	ND	ND
	Jan. 2004	ND	ND	ND	ND
	Oct. 2004	470	460	−8	98

Note: Timing as described in legend of Table 1

[a] Positive flux indicates transport from sediment to water column

[b] ND: not determined

Source: Data kindly provided by Sophie Tankere-Muller, Lancaster University, Lancaster, UK

Metal Toxicity Tests with Aerobic Heterotrophic Isolates

In order to establish whether the deposition of metal-polluted sediment would increase the number of metal-resistant bacteria, heterotrophic isolates from mesocosms HBC, IFC, and IFD were subjected to metal toxicity tests in October 2004. Figure 2 shows the results of these toxicity assays on collections of 30, 21, and 23 isolates originating from HBC, IFC, and IFD, respectively. In the case of Cu toxicity (Fig. 2A), it was observed that only a modest fraction of isolates from mesocosms HBC and IFD showed resistance [i.e., a zone smaller than 5 mm (9% and 8%, respectively, of all isolates in each collection]. For mesocosms IFC and IFD, the highest fraction of bacteria exhibited inhibition zones between 6 and 11 mm (54 and 70%), whereas the majority of isolates from mesocosm HBC (57%) actually turned out to be rather sensitive to Cu. In addition, the number of Cu-sensitive bacteria in IFC was significantly lower than in IFD.

Figure 2B shows similar tests with Cd as the toxic agent. The majority of isolates from each mesocosm (HBC: 50%; IFC: 51%; and IFD: 91%) showed a zone smaller than 5 mm (i.e., relatively resistant against Cd). The second category (6–11 mm) comprised most of the other isolates (HBC: 43%; IFC: 39%; and IFD: 8%). Bacteria sensitive to Cd (zones larger than 12 mm) comprised 6% and 9% of the isolate collections from HBC and IFC, respectively, and were not detected at all in the isolate collection of mesocosm IFD. The number of Cd-tolerant bacteria in IFD sediment was higher than in IFC.

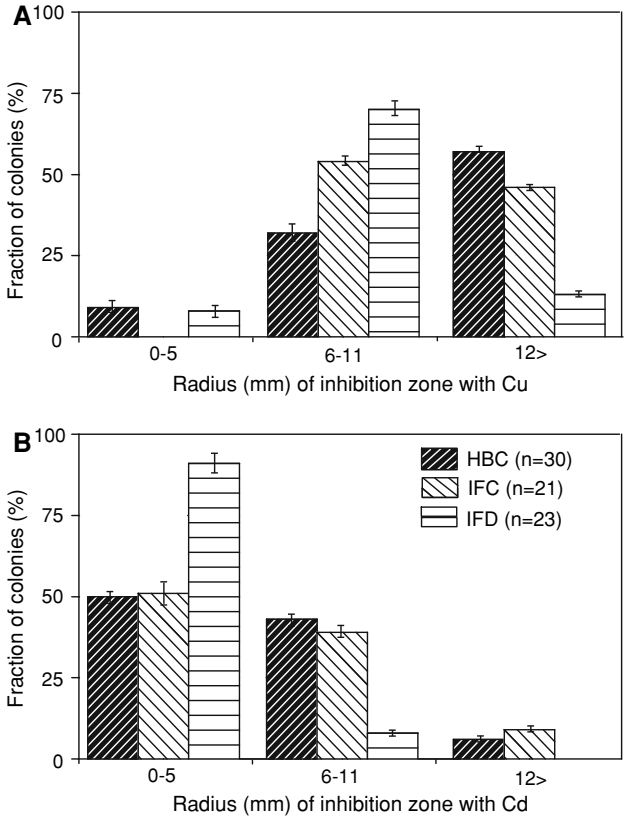

Fig. 2 Results from toxicity tests on collections of aerobic heterotrophs for Cu **(A)** and Cd **(B)**. Symbols shown are valid for both graphs. Metal toxicity was estimated by measuring zones of growth inhibition on agar plates amended with filter disks impregnated with Cu or Cd. Error bars represent standard deviation between two replicate experiments

DGGE Profiles of Sediment Samples and Statistical Analyses

To monitor major changes in the microbial communities during mesocosm incubation, DGGE profiles were constructed of the original sediments (HB and IF) and mesocosm samples taken at three different time points. Figure 3 shows the DGGE results for Bacteria (Fig. 3A), Archaea (Fig. 3B), and Cyanobacteria/chloroplasts (Fig. 3C). The average number of bands observed per DGGE profile and the total number of bands detected per DGGE gel were as follows: for Bacteria, 11.7/164 (Fig. 3A), for Archaea, 14.6/ 205 (Fig. 3B), and for Cyanobacteria, 12.1/ 170 (3C). As visual interpretation of DGGE patterns appeared to be rather subjective, a statistical tool was used to estimate profile similarity (Schauer et al. 2000). Results of nonmetric MDS analyses are shown in Figure 4 for Bacteria (Fig. 4A), Archaea (Fig. 4B), and Cyanobacteria (Fig. 4C). Figure 4D shows the results of cluster analysis of the sediment samples, combining information of the three above-mentioned groups.

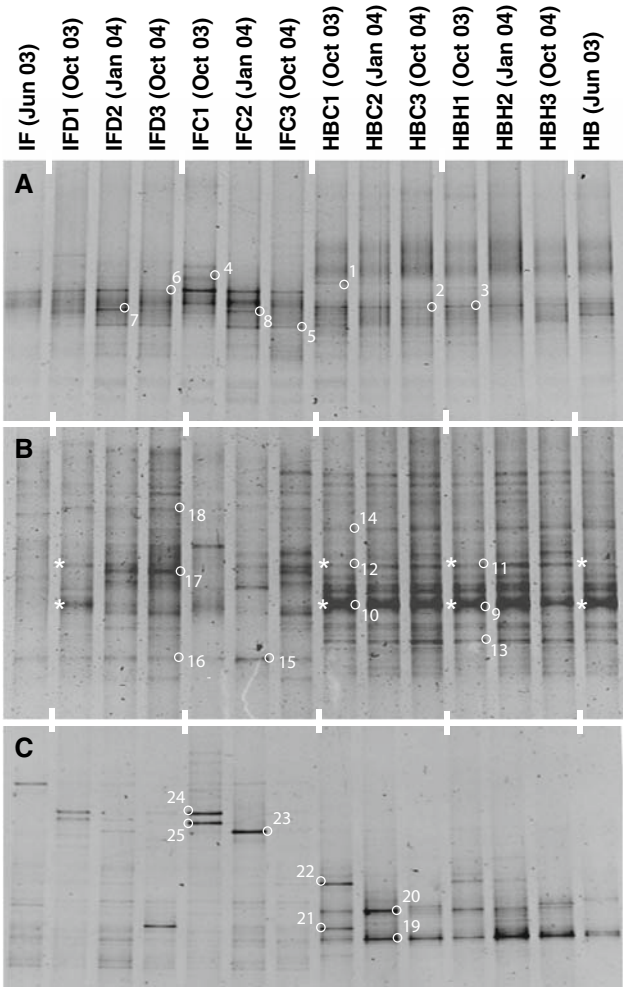

Fig. 3 DGGE profiles of bacterial **(A)**, archaeal **(B)**, and cyanobacterial **(C)** communities at different time intervals in the mesocosms during incubation. Legend above DGGE gel 3A is valid for all graphs. In addition to the previously described sampling points (Oct. 2003, Jan. 2004, and Oct. 2004), the outermost left lane shows DGGE profiles of the original IF sediment as sampled June 2003 (labeled IF) and the lane to the far right shows the original profiles for the harbor sediment (labeled HB). Open circles with numbers depict excised identified bands. DGGE bands marked with asterisks are discussed in the main text

The bacterial community profile showed many faint bands. Effects on community structure seemed minimal; the DGGE band patterns did not change much, even after transition from the sampling site to the mesocosms in the laboratory (lanes IF, IFD_1, and IFC_1 for the sandy sediment and lanes HB, HBC_1, and HBH_1 for the harbor sediment). For statistical analysis of DGGE profiles, the stress value of the analysis was lowest for the bacterial community (0.09) (i.e., the statistical significance was highest). Figure 4A shows that there was a tight relationship among all samples from the harbor sediments (HB, HBC_1-HBH_3). Subsequent cluster analysis revealed that the 50% similarity criterion also applied to the collection of sandy sediments (IF, IFC_1-IFD_3).

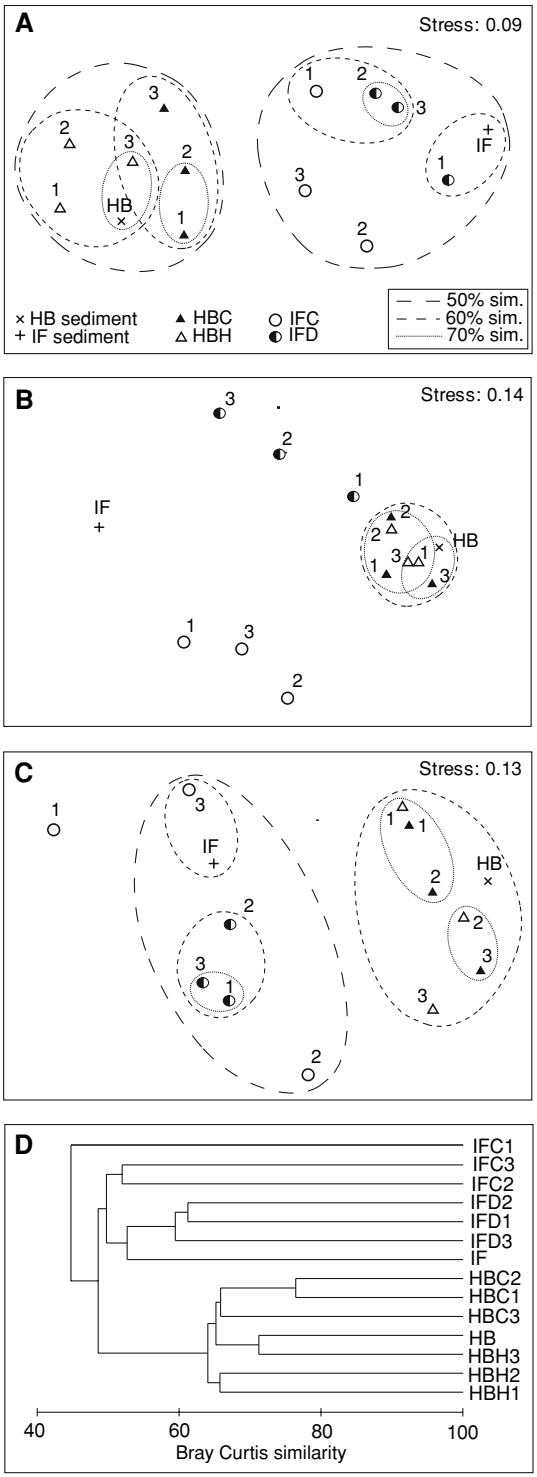

Fig. 4 Nonmetric MDS analyses of DGGE profiles of Bacteria **(A)**, Archaea **(B)**, and Cyanobacteria **(C)** and cluster analysis of all three groups combined **(D)**. Symbols shown in the top graph are valid for all graphs. MDS analyses received an overlay of Bray-Curtis resemblance, resulting in clustering according to 50%, 60%, or 70% similarity

Archaeal DGGE profiles showed a very stable community (Fig. 3B) in the case of the harbor sediments (HB, HBC_1-HBH_3). More variation in the number and positions

of bands was found in samples from the sandy sediments. IFD_1 and IFC_1 showed little similarity and the most dominant two bands in IFD_1 were at the same apparent height as major bands in HB, HBC, and HBH (denoted with an asterisk). IFC_3 and IFD_3 showed similar profiles again after 6 months of incubation. MDS analyses (Fig. 4B) confirmed these observations, as a strong clustering (within 60%) is seen for the harbor sediments (HB, HBC_1-HBH_3), whereas no significant clustering was found among the IF samples. However, sample IFD_1, taken directly after deposition of metal-polluted mud, was closer to the HB samples, whereas samples IFD_2 and IFD_3 indicated a trend toward IF.

Figure 3C depicts DGGE analysis of cyanobacterial fragments and revealed major differences in the phototrophic communities of the sandy and the harbor sediment. The latter showed profiles of modest diversity (lanes HB, HBC_1–HBH_3) with almost identical succession patterns. A closer look at the profiles in lanes IF and IFC_1–IFD_3 revealed a vast quantity of bands and also showed comparable successive changes in the two sandy sediments (IFC_1, IFC_2, IFD_1, and IFD_2). MDS analysis of the cyanobacterial gel (Fig. 4C) yielded a clear separation between HB and IF. Samples from mesocosm IFC showed the most variation, especially IFC_1 and IFC_2. The last graph, combining three DGGE profiles (Fig. 4D), depicts $IFD_{1–3}$ and the original sandy sediment (IF) on the same branch, despite the deposition of harbor mud. The samples from the sandy control sediment (IFC) form an outgroup, whereas all HB profiles were very similar and clustered together.

Phylogenetic Analysis of DGGE Bands

Most DGGE fragments that were sequenced belonged to the δ-Proteobacteria (bands 2, 3, 5, 7, and 8). Other bands were identified as members of the α-Proteobacteria (band 4), the Bacteroidetes (band 6), and a possible member of candidate division OPB46, associated to the *Haloanaerobiales* (band 1). These sequences and all other DGGE bands are represented in the phylogenetic tree in Figure 5. The main tree in the center shows different lineages present in the sediment samples, whereas the smaller trees depict a detailed view of phylogenetic diversity. All retrieved sequences from the Archaea were closely related (94–99% similarity) to other environmental sequences deposited at GenBank. One of the most intense bands in IFD_3 (i.e., band 17) belonged to the *Crenarcheota* and was related to the recently isolated ammonia-oxidizing *Nitrosopumilus maritimus* (AY351983). All other bands originated from sequences within the *Euryarchaeota*, with closely related to clones from various marine sediments (bands 9–16 and 18).

Cyanobacteria were found as major representatives of the phototrophic community in harbor sediments, as dominant bands were related to *Synechococcus* sp. (bands 19 and 21), *Spirulina subsalsa* (band 22), and *Pleurocapsa minor* (band 20). In contrast, DGGE analysis of the sandy mesocosms (IFC and IFD) showed the prevalence of mostly diatoms, with all three sequenced bands closely related (95–97% similarity) to chloroplast rRNA of *Amphora delicatissima*.

Screening of Bacterial Clone Libraries and Comparative Analyses

In order to facilitate a more detailed analysis of bacterial diversity and to verify whether any overlap existed between bacterial communities in the different mesocosms, possibly indicating carryover of bacteria as a consequence of sediment deposition, a more robust technique than DGGE was required. Therefore, clone libraries were made of nearly complete 16S rRNA genes amplified with target DNA extracted from mesocosm HBC (HBC_2 from May 2004 and HBC_3 from October 2004) and from mesocosm IFD (IFD_3 from October 2004). As a screening method, 38 (HBC_2), 101 (HBC_3), and 101 (IFD_3) positive clones were subjected to restriction analysis. Clustering of all clonal restriction patterns resulted in 26 ARDRA groups, 10 of which were detected in HBC_2, 18 in HBC_3, and 15 in IFD_3. Representative clones of each ARDRA group, 69 in total, were selected for complete sequencing of the small subunit ribosomal gene. These sequences were also included in Figure 5. From the sequences and their assigned ARDRA clusters, it can be derived that in most cases, sequence similarity within ARDRA groups varied from 90% to 99%, although few clusters did not meet this criterion (i.e., groups 5, 10, and 26).

About one-third of each library consisted of sequences that were most closely related to uncultured microorganisms according to similarity analysis with sequences stored in GenBank. The majority of sequences were affiliated to the Bacteroidetes (Fig. 5) (i.e., 71% of all clones in HBC_2, 47% in HBC_3, and 49% in IFD_3). The second most abundant were sequences related to the Proteobacteria, in particular to the γ- and the α-subclasses (11% and 13% for HBC_2, 21% and 17% for HBC_3, and 19% and 28% for IFD_3, respectively). The δ-subdivision of the Proteobacteria made up only a small fraction of the bacterial community in each library, namely 5% for HBC_2, 1% for HBC_3, and 5% for IFD_3. The remaining 16S rRNA sequences (HBC_3) were distantly affiliated to the phyla *Haloanaerobiales* and the *Acidobacteria*, clustering with sequences in candidate divisions JS1 and OP8, representing 9% and 6%, respectively.

Because differences in sample size (number of clones analyzed with ARDRA) and sequencing effort (ratio of

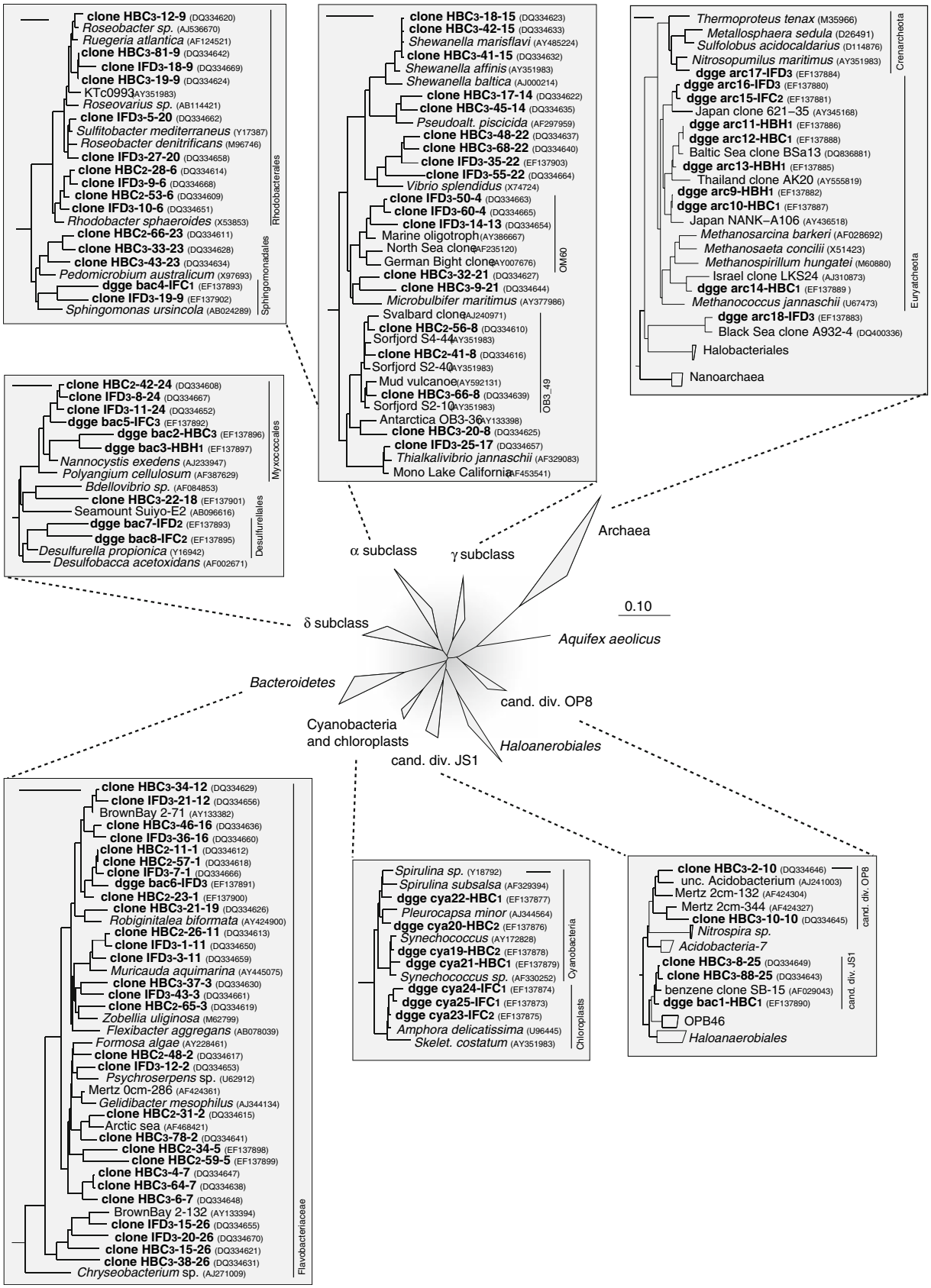
clone HBC3-12-9 (DQ334620)
Roseobacter sp. (AJ536670)
Ruegeria atlantica (AF124521)
clone HBC3-81-9 (DQ334642)
clone IFD3-18-9 (DQ334669)
clone HBC3-19-9 (DQ334624)
KTc0993 (AY351983)
Roseovarius sp. (AB114421)
clone IFD3-5-20 (DQ334662)
Sulfitobacter mediterraneus (Y17387)
Roseobacter denitrificans (M96746)
clone IFD3-27-20 (DQ334658)
clone HBC2-28-6 (DQ334614)
clone IFD3-9-6 (DQ334668)
clone HBC2-53-6 (DQ334609)
clone IFD3-10-6 (DQ334651)
Rhodobacter sphaeroides (X53853)
clone HBC2-66-23 (DQ334611)
clone HBC3-33-23 (DQ334628)
clone HBC3-43-23 (DQ334634)
Pedomicrobium australicum (X97693)
dgge bac4-IFC1 (EF137893)
clone IFD3-19-9 (EF137902)
Sphingomonas ursincola (AB024289)
Rhodobacterales
Sphingomonadales
clone HBC3-18-15 (DQ334623)
clone HBC3-42-15 (DQ334633)
Shewanella marisflavi (AY485224)
clone HBC3-41-15 (DQ334632)
Shewanella affinis (AY351983)
Shewanella baltica (AJ000214)
clone HBC3-17-14 (DQ334622)
clone HBC3-45-14 (DQ334635)
Pseudoalt. piscicida (AF297959)
clone HBC3-48-22 (DQ334637)
clone HBC3-68-22 (DQ334640)
clone IFD3-35-22 (EF137903)
clone IFD3-55-22 (DQ334664)
Vibrio splendidus (X74724)
clone IFD3-50-4 (DQ334663)
clone IFD3-60-4 (DQ334665)
clone IFD3-14-13 (DQ334654)
Marine oligotroph (AY386667)
North Sea clone (AF235120)
German Bight clone (AY007676)
clone HBC3-32-21 (DQ334627)
clone HBC3-9-21 (DQ334644)
Microbulbifer maritimus (AY377986)
Svalbard clone (AJ240971)
clone HBC2-56-8 (DQ334610)
Sorfjord S4-44 (AY351983)
clone HBC2-41-8 (DQ334616)
Sorfjord S2-40 (AY351983)
Mud vulcanoe (AY592131)
clone HBC3-66-8 (DQ334639)
Sorfjord S2-10 (AY351983)
Antarctica OB3-36 (AY133398)
clone HBC3-20-8 (DQ334625)
clone IFD3-25-17 (DQ334657)
Thialkalivibrio jannaschii (AF329083)
Mono Lake California (AF453541)
OM60
OB3_49
Thermoproteus tenax (M35966)
Metallosphaera sedula (D26491)
Sulfolobus acidocaldarius (D114876)
Nitrosopumilus maritimus (AY351983)
dgge arc17-IFD3 (EF137884)
dgge arc16-IFD3 (EF137880)
dgge arc15-IFC2 (EF137881)
Japan clone 621–35 (AY345168)
dgge arc11-HBH1 (EF137886)
dgge arc12-HBC1 (EF137888)
Baltic Sea clone BSa13 (DQ836881)
dgge arc13-HBH1 (EF137885)
Thailand clone AK20 (AY555819)
dgge arc9-HBH1 (EF137882)
dgge arc10-HBC1 (EF137887)
Japan NANK–A106 (AY436518)
Methanosarcina barkeri (AF028692)
Methanosaeta concilii (X51423)
Methanospirillum hungatei (M60880)
Israel clone LKS24 (AJ310873)
dgge arc14-HBC1 (EF137889)
Methanococcus jannaschii (U67473)
dgge arc18-IFD3 (EF137883)
Black Sea clone A932-4 (DQ400336)
Halobacteriales
Nanoarchaea
Crenarcheota
Euryatcheota
clone HBC2-42-24 (DQ334608)
clone IFD3-8-24 (DQ334667)
clone IFD3-11-24 (DQ334652)
dgge bac5-IFC3 (EF137892)
dgge bac2-HBC3 (EF137896)
dgge bac3-HBH1 (EF137897)
Nannocystis exedens (AJ233947)
Polyangium cellulosum (AF387629)
Bdellovibrio sp. (AF084853)
clone HBC3-22-18 (EF137901)
Seamount Suiyo-E2 (AB096616)
dgge bac7-IFD2 (EF137893)
dgge bac8-IFC2 (EF137895)
Desulfurella propionica (Y16942)
Desulfobacca acetoxidans (AF002671)
Myxococcales
Desulfurellales
α subclass
γ subclass
Archaea
0.10
δ subclass
Aquifex aeolicus
Bacteroidetes
cand. div. OP8
Cyanobacteria
and chloroplasts
Haloanerobiales
cand. div. JS1
clone HBC3-34-12 (DQ334629)
clone IFD3-21-12 (DQ334656)
BrownBay 2-71 (AY133382)
clone HBC3-46-16 (DQ334636)
clone IFD3-36-16 (DQ334660)
clone HBC2-11-1 (DQ334612)
clone HBC2-57-1 (DQ334618)
clone IFD3-7-1 (DQ334666)
dgge bac6-IFD3 (EF137891)
clone HBC2-23-1 (EF137900)
clone HBC3-21-19 (DQ334626)
Robiginitalea biformata (AY424900)
clone HBC2-26-11 (DQ334613)
clone IFD3-1-11 (DQ334650)
clone IFD3-3-11 (DQ334659)
Muricauda aquimarina (AY445075)
clone HBC3-37-3 (DQ334630)
clone IFD3-43-3 (DQ334661)
clone HBC2-65-3 (DQ334619)
Zobellia uliginosa (M62799)
Flexibacter aggregans (AB078039)
Formosa algae (AY228461)
clone HBC2-48-2 (DQ334617)
clone IFD3-12-2 (DQ334653)
Psychroserpens sp. (U62912)
Mertz 0cm-286 (AF424361)
Gelidibacter mesophilus (AJ344134)
clone HBC2-31-2 (DQ334615)
Arctic sea (AF468421)
clone HBC3-78-2 (DQ334641)
clone HBC2-34-5 (EF137898)
clone HBC2-59-5 (EF137899)
clone HBC3-4-7 (DQ334647)
clone HBC3-64-7 (DQ334638)
clone HBC3-6-7 (DQ334648)
BrownBay 2-132 (AY133394)
clone IFD3-15-26 (DQ334655)
clone IFD3-20-26 (DQ334670)
clone HBC3-15-26 (DQ334621)
clone HBC3-38-26 (DQ334631)
Chryseobacterium sp. (AJ271009)
Flavobacteriaceae
Spirulina sp. (Y18792)
Spirulina subsalsa (AF329394)
dgge cya22-HBC1 (EF137877)
Pleurocapsa minor (AJ344564)
dgge cya20-HBC2 (EF137876)
Synechococcus (AY172828)
dgge cya19-HBC2 (EF137878)
dgge cya21-HBC1 (EF137879)
Synechococcus sp. (AF330252)
dgge cya24-IFC1 (EF137874)
dgge cya25-IFC1 (EF137873)
dgge cya23-IFC2 (EF137875)
Amphora delicatissima (U96445)
Skelet. costatum (AY351983)
Cyanobacteria
Chloroplasts
clone HBC3-2-10 (DQ334646)
unc. Acidobacterium (AJ241003)
Mertz 2cm-132 (AF424304)
Mertz 2cm-344 (AF424327)
clone HBC3-10-10 (DQ334645)
Nitrospira sp.
Acidobacteria-7
clone HBC3-8-25 (DQ334649)
clone HBC3-88-25 (DQ334643)
benzene clone SB-15 (AF029043)
dgge bac1-HBC1 (EF137890)
OPB46
Haloanaerobiales
cand. div. OP8
cand. div. JS1

◀ **Fig. 5** 16S rRNA neighbor-joining tree of the domains Bacteria and Archaea containing 69 sequences obtained from 3 clone libraries (HBC_2, HBC_3, and IFD_3) and 25 excised DGGE bands, in addition to sequences from the ARB database (84 mostly full-length sequences). The backbone tree was constructed without correction, using *E. coli* as a filter and rooted with *Aquifex aeolicus*. The phylogenetic affiliation of sequences from this study (**bold**) is depicted in more detail in the smaller subtrees. These subtrees were derived from the same sequence alignment, but scaled differently, showing individual clones (**library name-clone number-ARDRA group**). All scale bars represent 0.10 changes per nucleotide

sequenced clones versus sample size) existed between libraries, different approaches were combined to estimate and compare diversity. WebLIBSHUFF analysis (Singleton et al. 2001) was selected for library comparison because it is independent of a strict species definition, but rather computes similarity across all possible cutoff values. Two libraries are considered significantly different when $p < 0.05$, as was the case in the comparison of HBC_3 to IFD_3 ($p = 0.001$). Notably, the p-value for the reverse comparisons was much higher ($p = 0.374$), indicating that sample IFD_3 did not contain many species that were not present in sample HBC_3. Analysis showed that HBC_2 was very similar to HBC_3 ($p = 0.783$). To further investigate differences in bacterial diversity between the different sites, richness estimators (Shannon (H') and Chao2) and coverage (C) were calculated, as summarized in Table 3. As a uniqueness criterion, a 16S rRNA gene similarity of <95% was applied. Sequences of three clusters in the *Bacteroidetes* (see Fig. 5) (i.e., ARDRA groups 3, 2, and 26) did not meet this criterion and all of their members were therefore counted as individuals.

Discussion

Metal Distribution in Mesocosm Sediments

The pore-water metal contents in the HB sediments were higher than in the IF sediments (Fig. 1), but similar to maximum concentrations observed in other sites throughout the North Sea and river sediments (BSH 2002), with the exception of Cu. However, pore-water Cu concentrations detected in mesocosm HBC in January 2004 were at least 50-fold higher, and 10-fold to 20-fold elevated, when compared to values in other North Sea sediments. This extreme Cu pollution is primarily connected to the fact that the HB is located in the vicinity of an industrial wharf (Schiff et al. 2004; Warnken et al. 2004).

Profiles of pore-water Cu and Cd concentrations (Figs. 1C–1F) peak at the surface or just below. High surface concentrations were probably caused by the microbial oxidation of metal-contaminated organics at the sediment surface (Tankere-Muller et al. 2007). Because oxygen penetration depth varied between different time points, the release of Cu and Cd in the subsurface (below 1 cm) could also be caused by the anaerobic reduction of heavy-metal-containing iron(hydr)oxides (Markwiese and Colberg 2000). After 3 months of bioturbation with *N. diversicolor*, Fe, Cu, and Cd pore-water concentrations were lowered approximately 10-fold at all sediment depths, due to mixing by the polychaete worms and subsequent chemical oxidation, adsorption, or precipitation.

Perception of Diversity

Clone libraries of 16S rRNA genes and DGGE analyses have been widely used to investigate microbial communities of different habitats, but these approaches suffer from specific limitations that have been elaborated on previously (LaMontagne et al. 2002; von Wintzingerode et al. 1997). Because this study does not aim to describe diversity in general, but focuses on specific changes in microbial diversity, the use of identical tools on different mesocosms minimizes variance in methodological biases. It is commonly accepted that only dominant populations (i.e., constituting more than 0.1–1% relative abundance) are detectable in DGGE profiles of complex microbial communities (Muyzer et al. 1993), whereas the detection limit of clone libraries depends solely on the number of clones that are analyzed. Contrastingly, the chance of obtaining a numerically dominant bacterium in isolation depends on

Table 3 Diversity indices and coverage as calculated from clone library data

Library	No. of clones	No. of ARDRA groups (unique)[a]	Coverage (%)[b,c]	Shannon (H′)[c]	Chao2 (95% CI)[c,d]
HBC_2	38	10 (1)	82.2	2.41	75 (36–182)
HBC_3	101	18 (8)	86.8	2.88	248 (137–470)
IFD_3	101	15 (4)	84.3	2.84	203 (111–396)

[a] Total number of ARDRA groups detected in clone library and number of unique ARDRA groups in parentheses

[b] Coverage was calculated with the equation of Good (1953)

[c] Coverage, Shannon index, and Chao2 estimator were calculated using the uniqueness definition of <95% 16S rRNA gene similarity

[d] The 95% confidence intervals are listed in parentheses

how well incubation conditions resemble the bacterial microenvironment. The concentration of the carbon source in the culture medium (5 mM) was high compared to TOC values in both the sandy and the muddy sediments and might have triggered opportunistic bacteria. The results obtained by the application of two molecular techniques and primer sets for the determination of bacterial diversity suggested agreement between the methods, as members of the δ-Proteobacteria, the Bacteroidetes, and candidate division JS1 were detected independently in both cases. The fact that community composition was not reflected by the collection of DGGE bands in the phylogenetic trees (Fig. 5) can partially be explained by the fact that not all bands within one profile could be identified. The high number of DGGE bands related to members of the δ-Proteobacteria is in contrast with the low abundance of this group according to clone library results (around 5%) and could indicate primer preferences.

Changes in Archaeal and Cyanobacterial Communities

The archaeal communities in mesocosms HBC and HBD showed a very stable composition during incubation time, whereas DGGE profiles from IFD and IFC were more variable (Figs. 3B and 4B). Sandaa and co-workers (1999b) detected a decrease in archaeal abundance and a shift in community composition in soils amended with heavy metals. In this study, the latter effect was only initially observed (IFD_1) and the similarity between DGGE profiles (Figs. 3B and 4B) increased again at the end of the experiment.

Cyanobacterial DGGE profiles (Fig. 3C) showed successive changes in the composition of the photosynthetic community in mesocosms IFC and IFD. These changes might be due to bioturbation, grazing pressure, or the shift from natural to artificial light conditions (daylight is 20 times stronger than the lamps used). The DGGE profiles were dominated by closely related strains of the diatom *Amphora delicatissima*. Contrastingly, DGGE profiles of mesocosms HBC and HBH revealed a simple and stable community structure consisting of *Synechococcus* sp. and *Pleurocapsa* sp. Lower flow rates during mesocosm incubation might have favored growth of the rather fragile diatoms in the sandy sediments (Stal 2003). Phytoplankton species in general are sensitive to Cu and other metals due to impairment of the photosynthetic electron transport system (Miao et al. 2005; Surosz and Palinska 2004). Although no attempts were made in this study to quantify the phototrophic biomass, oxygen flux measurements at the sediment–water interface in mesocosm IFD confirmed this sensitivity by showing a steep decline in oxygen production immediately after the addition of metal-polluted sludge.

Changes in Bacterial Communities

Changes in bacterial diversity as a result of the deposition of metal-polluted sediment were not readily observed in the DGGE profiles (Fig. 3A). Comparative analysis between clone libraries HBC_3 and IFD_3 showed several groups of highly similar, but not identical clones. These "shared" clusters were most closely related to *Ruegeria atlantica*, *Rhodobacter sphaeroides*, *Vibrio splendidus*, and a group related to environmental clone BrownBay 2–71, within the *Flavobacteriaceae* (Fig. 5). Particularly, this latter group showed high 16S rRNA gene similarities between clones from IFD_3 and HBC_3 (ARDRA group 12: 99% similarity; and group 16: 98%). Interestingly, clone BrownBay 2–71 actually originated from a heavy-metal-polluted Antarctic sediment (Powell et al. 2003). Statistical comparisons between the clone libraries showed that the bacterial community in sediment HBC_3 was significantly different from IFD_3 ($p = 0.001$). Diversity estimators (Table 3) indicated HBC_3 as having the highest species richness, although differences with IFD_3 were very small. A similar trend was observed in Antarctic sediments when comparing clone libraries of polluted and pristine sites (Powell et al. 2003). This high diversity might be related to the fact that metal-polluted environments usually also contain many other types of contaminant, such as petroleum hydrocarbons or chlorinated compounds, in addition to increased concentrations of organics and nutrients. Therefore, in an environment poor in organic carbon and nutrients, the selective pressure presumably exerted by heavy metals might be overshadowed by a diversity increase, due to expanding metabolic possibilities.

Effects of Sediment Homogenization and Redeposition

Homogenization of metal-polluted sediment (HBH) was expected to cause a temporary decrease of metal concentrations in pore waters, due to trapping of metal ions by previously buried sulfides or due to adsorption to freshly formed iron oxides (Markwiese and Colberg 2000). In this study, only small, localized effects were observed for Cu and Cd after sediment homogenization (Fig. 1). Concomitantly, a small fraction of organic carbon was oxidized and ammonia was released (Table 1). A study on the environmental effects of dredging activities in the Pongol estuary, Singapore (Nayar et al. 2007) also showed elevated levels of ammonia and depletion of organic carbon during and after sediment removal. The effects of homogenization on metal concentrations observed in this study were in accordance with earlier findings (van den Berg et al. 2000). No important changes were observed in the microbial communities of HB sediments after sediment homogenization and incubation

(Figs. 3 and 4), indicating that similar microorganisms were present throughout the sediment column and that the dominant consortium was not influenced by small-scale disturbances. This observation was in sharp contrast to the mesocosms with sandy sediments, which, overall, showed more heterogeneity and temporal fluctuations.

Deposition of a 3-mm layer of metal-polluted sediment on a sandy sediment (IFD) caused a substantial increase in pore-water Cu concentrations of surface sediments (4-fold compared to IFC and 1.5-fold compared to HBC) and led to significant metal fluxes from sediment to water column (Fig. 1, Tables 1 and 2). All of these effects were of a transient nature and had mostly disappeared after 1 year of mesocosm incubation. Elevated pore-water metal concentrations as a result of redeposition of polluted sediment were also described in other studies (Leipe et al. 2005). However, the degree of impact depends on the volume of deposited material and its contamination level, as Chen and co-authors (2003) only observed an increase in Cu levels after deposition of a 5-cm layer of polluted sediment, whereas no effects could be detected underneath a 1-cm layer.

Toxicity tests with isolates underlined the effects of the deposition of metal-polluted sediment by showing a substantial increase in Cu- and Cd-tolerant aerobic heterotrophs from mesocosm IFD when compared to IFC. The fraction of Cd-tolerant bacteria in IFD was even higher than observed for isolates of mesocosm HBC (Fig. 2). In addition, the collection bacteria from IFD contained the lowest percentage of Cu- and Cd-sensitive bacteria. Elevated levels of metal-tolerant Bacteria in soils and sediments after exposure to heavy metals have been described previously (Diaz-Ravina and Baath 1996; Ramaiah and De 2003; Rasmussen and Soerensen 1998), but not in combination with detailed metal analyses indicating such localized and short-term metal exposure.

In conclusion, this study provides convincing evidence for a prolonged modification of the indigenous bacterial community caused by transient exposure to Cu and Cd. It seems unlikely that this adaptation concerns numerically dominant microorganisms, as large community shifts were not observed in DGGE profiles, except, initially, for the archaeal population. It remains to be determined whether the increase in metal resistance in mesocosm IFD is due to the proliferation of metal-tolerant bacteria, originating from the deposited metal-polluted sediment, or whether horizontal gene transfer of metal-resistance genes might have played a role.

Acknowledgments This research was funded by the 5th framework directive European Union project TREAD (EVK-CT-2002–00081). The authors would like to acknowledge the scientific partners in this project for informative discussions and especially Sophie Tankere-Muller, Hao Zhang, and Bill Davison from Lancaster University for their expertise concerning metal dynamics. Additionally, the practical assistance of Esengül Yildirim, Carmen Gonzalez-Domenech, and Vioryca Picioreanu was much appreciated. Finally, we would like to thank Robert Colwell (Department of Ecology & Evolutionary Biology, University of Connecticut) and James Henriksen (Department of Microbiology, University of Georgia) for their suggestions and recommendations concerning the statistical tools.

References

Altschul SF, Gish W, Miller W, Myers EW, Lipman DJ (1990) Basic local alignment search tool. J Mol Biol 215:403–410

Bortone G, Arevalo E, Deibel I et al (2004) Sediment and dredged material treatment. J Soil Sed 4:225–232

BSH (Bundesamt für Seeschifffahrt und Hydrographie) (2002) Bund/Länder-Messprogramm: Messprogramm Meeresumwelt; Zustandsbericht, 1997–1998 für Nordsee und Ostsee. Hamburg Rostock, Hamburg p 176

Chen Y-X, Zhu G-W, Tian G-M, Chen H-L (2003) Phosphorus and copper leaching from dredged sediment applied on a sandy loam soil: column study. Chemosphere 53:1179–1187

Cook MA, Osborn AM, Bettandorff J, Sobecky PA (2001) Endogenous isolation of replicon probes for assessing plasmid ecology of marine sediment microbial communities. Microbiology 147:2089–2101

Coolen MJL, Hopmans EC, Rijpstra WIC et al (2004) Evolution of the methane cycle in Ace Lake (Antarctica) during the Holocene: response of methanogens and methanotrophs to environmental changes. Org Geochem 35:1151–1167

De Beer D, Wenzhofer F, Ferdelman TG et al (2005) Transport and mineralization rates in North Sea sandy intertidal sediments, Sylt-Romo Basin, Wadden Sea. Limnol Oceanogr 50:113–127

Diaz-Ravina M, Baath E (1996) Development of metal tolerance in soil bacterial communities exposed to experimentally increased metal levels. Appl Environ Microbiol 62:2970–2977

EEA (European Environmental Agency) (2003) Trends in metals and persistent organic pollutants. In: Green N, Bjerkeng B, Hylland K, Ruus A, Rygg B (eds) Hazardous substances in the European marine environment. Norwegian Institute for Water Research, Copenhagen, pp 0–85

Ferdelmann TG, Lee C, Pantoja S, Harder J, Bebout BM, Fossing H (1997) Sulfate reduction and methanogenesis in Thioploca-dominated off the coast of Chile. Geochem Cosmochim Acta 61:3065–3079

Gillan DC, Danis B, Pernet P, Joly G, Dubois P (2005) Structure of sediment-associated microbial communities along a heavy-metal contamination gradient in the marine environment. Appl Environ Microbiol 71:679–690

Good IJ (1953) The population frequencies of species and the estimation of population parameters. Biometrika 40:237–262

Hansen HP, Koroleff F (1999) Determination of nutrients. In: Grasshoff K, Kremling K, Ehrhard M (eds) Methods of seawater analysis. Wiley-VCH, Berlin, pp 159–229

LaMontagne MG, Michel J, FC, Holden PA, Reddy CA (2002) Evaluation of extraction and purification methods for obtaining PCR-amplifiable DNA from compost for microbial community analysis. J Microbiol Methods 49:255–264

Leipe T, Kersten M, Heise S et al (2005) Ecotoxicity assessment of natural attenuation effects at a historical dumping site in the western Baltic Sea. Marine Pollut Bull 50:446–459

Ludwig W, Strunk O, Westram R et al (2004) ARB: a software environment for sequence data. Nucleic Acids Res 32:1363–1371

Marchesi JR, Weightman AJ (2000) Modified primers facilitate rapid screening of 16S rRNA gene libraries. Biotechniques 29:48–50

Markwiese JT, Colberg PJS (2000) Bacterial reduction of copper-contaminated ferric oxide: copper toxicity and the interaction between fermentative and iron-reducing bacteria. Arch Environ Contam Toxicol 38:139–146

Miao A-J, Wang W-X, Juneau P (2005) Comparison of Cd, Cu, and Zn toxic effects on four marine phytoplankton by pulse-amplified-modulated fluorometry. Environ Toxicol Chem 24:2603–2611

Muyzer G, de Waal EC, Uitterlinden AG (1993) Profiling of complex microbial populations by denaturing gel electrophoresis analysis of polymerase chain reaction-amplified genes coding for 16S rRNA. Appl Environ Microbiol 59:695–700

Musat N, Werner U, Knittel K et al (2006) Microbial community structure of sandy intertidal sediments in the North Sea, Sylt-Romo Basin, Wadden Sea. Syst Appl Microbiol 29:333–348

Nayar S, Miller DJ, Hunt A, Goh BPL, Chou LM (2007) Environmental effects of dredging on sediment nutrients, carbon and granulometry in a tropical estuary. Environ Monit Assess 127:1–13

Nies DH (1999) Microbial heavy-metal resistance. Appl Microbiol Biotechnol 51:730–750

Nubel U, Garcia-Pichel F, Muyzer G (1997) PCR primers to amplify 16S rRNA genes from cyanobacteria. Appl Environ Microbiol 63:3327–3332

Powell SM, Bowman JP, Snape I, Stark JS (2003) Microbial community variation in pristine and polluted nearshore Antarctic sediments. FEMS Microbiol Ecol 45:135–145

Ramaiah N, De J (2003) Unusual rise in mercury-resistant bacteria in coastal environs. Microb Ecol 45:444–454

Rasmussen LD, Soerensen SJ (1998) The effect of long-term exposure to mercury on the bacterial community in marine sediment. Curr Microbiol 36:291–197

Sandaa R-A, Torsvik V (1999a) Analysis of bacterial communities in heavy metal-contaminated soils at different levels of resolution. FEMS Microbiol Ecol 30:237–251

Sandaa R-A, Enger Ö, Torsvik V (1999b) Abundance and diversity of Archaea in heavy metal-contaminated soils. Appl Environ Microbiol 65:3293–3297

Schäfer H, Muyzer G (2001) Denaturing gradient gel electrophoresis in marine microbial ecology. In: Paul JH (ed) Methods in microbiology, Vol. 30. Academic Press, St. Petersburg, FL

Schauer M, Massana R, Pedros-Alio C (2000) Spatial differences in bacterioplankton composition along the Catalan coast (NW Mediterranean) assessed by molecular fingerprinting. FEMS Microbiol Ecol 33:51–59

Schiff K, Diehl D, Valkirs A (2004) Copper emissions from antifouling paint on recreational vessels. Marine Pollut Bull 48:371–377

Silver S (1996) Bacterial resistances to toxic metal ions: a review. Gene 179:9–19

Singleton DR, Furlong MA, Rathbun SL, Whitman WB (2001) Quantitative comparisons of 16S rRNA gene sequence libraries from environmental samples. Appl Environ Microbiol 67:4374–4376

Sobecky PA, Mincer TJ, Chang MC, Toukdarian A, Helinski DR (1998) Isolation of broad-host-range replicons from marine sediment bacteria. Appl Environ Microbiol 64:2822–2830

Sorci JJ, Paulauskis JD, Ford TE (1999) 16S rRNA restriction fragment length polymorphism analysis of Bacterial diversity as a biomarker of ecological health in polluted sediments from New Bedford Harbor, Massachusetts, USA. Marine Pollut Bull 38:663–675

Stal LJ (2003) Microphytobenthos, their extracellular polymeric substances, and the morphogenesis of intertidal sediments. Geomicrobiol J 20:463–478

Surosz W, Palinska KA (2004) Effects of heavy-metal stress on cyanobacterium *Anabaena flos-aquae*. Arch Environ Contam Toxicol 48:40–48

Tankere-Muller S, Zhang H, Davison W et al (2007) Fine scale remobilisation of Fe, Mn, Co, Ni, Cu and Cd in contaminated marine sediment. Marine Chem 106(1–2):192–207

Van den Berg GA, Meijers GGA, Van der Heijdt LM, Zwolsman JJG (2001) Dredging-related mobilisation of trace metals: a case study in The Netherlands. Water Res 35:1979–1986

von Wintzingerode F, Gobel UB, Stackebrandt E (1997) Determination of microbial diversity in environmental samples: pitfalls of PCR-based rRNA analysis. FEMS Microbiol Rev 21:213–229

Wang Q, Kim D, Dionysiou DD, Sorial GA, Timberlake D (2004) Sources and remediation for mercury contamination in aquatic systems: a literature review. Environ Pollut 131:323–336

Warnken J, Dunn RJK, Teasdale PR (2004) Investigation of recreational boats as a source of copper at anchorage sites using time-integrated diffusive gradients in thin film and sediment measurements. Marine Pollut Bull 49:833–843

Widdel F, Pfennig N (1984) Dissimilatory sulfate- or sulfur-reducing bacteria. In: Krieg NR, Holt JD (eds) Bergey's manual of systematic bacteriology, Vol. 1. The Williams & Wilkins Co., Baltimore, pp 663–679

Zhang H, Davison W (1999) Diffusional characteristics of hydrogels used in DGT and DET techniques. Anal Chim Acta 398:329–340

Zhang H, Davison W, Miller S, Tych W (1995) In situ high resolution measurements of fluxes of Ni, Cu, Fe and Mn and concentrations of Zn and Cd in porewaters by DGT. Geochim Cosmochim Acta 59:4181–4192